WIND TUNNEL MODEL VALIDATION FOR VAPOR DISPERSION FROM VAPOR DETENTION SYSTEM

by

Seong-Hee Shin and Robert N. Meroney
Colorado State University

Ted Williams
Gas Research Institute

Fluid Mechanics and Wind Engineering Program
Department of Civil Engineering
Colorado State University
Fort Collins, Colorado 80523

Prepared for
International Conference and Workshop
on Modeling & Mitigating the Consequences of
Accidental Releases of Hazardous Materials
New Orleans, Louisiana
May 21-24, 1991

November 1990

CEP90-91-SHS-RNM9

WIND TUNNEL MODEL VALIDATION FOR VAPOR DISPERSION FROM VAPOR DETENTION SYSTEM

Seong-Hee Shin and Robert N. Meroney
Colorado State University, Fort Collins, USA
Ted Williams
Gas Research Institute

ABSTRACT This paper summarizes wind tunnel simulations of the Falcon Series large scale LNG spill experiments conducted at the Nevada test site by Lawrence Livermore National Laboratory (LLNL) in 1987. Detailed comparisons of field data and wind tunnel simulations at different model length scales and using different simulant gases are addressed.

1. Introduction

Dispersion of liquefied natural gas (LNG) in the event of an accidental spill is a major concern in LNG storage safety planning, hazard response, and facility siting. Field experiments were planned by the LLNL for the Department of Transportation (DOT) and the Gas Research Institute (GRI) as part of a joint government/industry study in 1987 [Brown et al., 1988] to evaluate the effectiveness of vapor fences as a mitigation technique for accidental release of LNG and to assist in validating wind tunnel and numerical methods for vapor dispersion simulation.

Post-field-spill wind-tunnel experiments were performed by Colorado State University [1988, 1989] to augment the LNG Vapor Fence Program data obtained during the Falcon Test Series. The program included four different model length scales and two different simulant gases. The purpose of this program is to provide a basis for the analysis of the simulation of physical modeling tests using proper physical modeling techniques and to assist in the development and verification of analytical models. Field data and model data are compared and analyzed statistically, pattern comparison factors are

calculated, and model data is compared with a layer-averaged numerical program to evaluate a vapor-barrier entrainment model.

2. Post-field Experimental Measurements

2.1 Post-field Tests

Sixteen different sets of post-field-spill tests were simulated in the Environmental Wind Tunnel (EWT) at Colorado State University at model length scales of 1:50, 1:100, 1:150, and 1:200 to examine the sensitivity of results to various scaling arguments. Each test was repeated 5 times to evaluate the reproducibility. Figure 1 displays the layout of the source area, the vortex generating barrier and the vapor fence. All dimensions shown are at field scale. Table 1 summarizes the post-field-spill tests conducted. The table specifies the array angle of the model and the percentages of source gas released from the modeled evaporating pond and spider respectively. Since field trials of Falcon Test Series had various meteorological conditions resulting in different concentration time histories at a fixed location for each run, an optimum combination of the model source gas supply from the modeled evaporating pond and the spider were selected prior to performing each set of post-field tests by referring to field data inside the fence. No downwind model/field data comparisons were made during definition of the source model. Pure Argon was used as a simulant gas for all test sets, and pure Freon-12 gas was used for the simulation of Falcon 4 with model scales of 1:150 and 1:200.

2.2 Concentration Measurement Technique

Concentration fluctuation measurements are necessary to predict flammable methane concentrations. Rapid concentration fluctuations found during small-scale laboratory simulations require concentration sensors with a rise-time of the order of a millisecond, and such a detector was designed and constructed by Neff [1986] at Colorado State University. A rack of eight hot-wire aspirating probes were manufactured to obtain the concentration time histories at points

downwind of the spill site. The Colorado State aspirated probe has a 60 Hz frequency response and this is well above the expected frequencies for concentration fluctuations in this test program. A 60 Hz frequency response for a model scale of 1:100 corresponds to 11 Hz at field scale. This is far above the 1 Hz frequency used in field tests.

3. Discussion

Field data and wind tunnel experiments were compared through surface pattern and statistical methods. A layer-averaged slab model developed by Meroney et al. [1988] (FENC23) was expanded to evaluate an enhanced entrainment model proposed for dense gas dispersion including the effect of vapor barriers.

3.1 Effect of Different Model Scales and Different Simulant Gases on Plume Similarity

Four different scales of models and two different simulant gases were used during the post-field laboratory experiments. Peak centerline concentrations, concentration time histories, and concentration contours from model data were compared to field data.

Figure 2 shows concentration time series observed at (X=150 m, Y=-28 m, Z=5 m) for all model scales and for the Falcon 4 test. Figure 3 displays peak array-centerline concentrations at Z=5 m for Falcon 4 simulations. The maximum value of peak concentrations observed during all repetitions were used for the plot. It is seen that the physical model data with length scale of 100 predicts the field data fairly well while other physical model scales generally underpredict peak concentrations.

The performance measures that are most relevant to evaluation of hazardous gas models have been considered by several researchers [Mercer, 1987; Ermak et al., 1988; Hanna et al., 1988]. The fractional bias (FB) and normalized mean square error (NMSE) defined by;

$$FB = (\bar{C}_m - \bar{C}_f) / [0.5(\bar{C}_m + \bar{C}_f)]$$

$$NMSE = \overline{(C_m - C_f)^2} / (\bar{C}_m \bar{C}_f)$$

were calculated, where an overbar indicates an average over all points in the data set. Data from post-field-spill experiments of Falcon 2, Falcon 3, and Falcon 4 tests were examined. All downwind data points ($X > 0$ m) were included, and concentration time histories from both field and model tests were averaged over the same time period (11 sec in field time). Data were analyzed for the magnitude of $\bar{C}_{MAX}$, the arrival time of concentration with a magnitude of 20 percent of $\bar{C}_{MAX}$, and the arrival time of $\bar{C}_{MAX}$.

Figure 4 provides a plot of NMSE vs. FB for peak concentration data. This figure shows that all laboratory tests underpredict the peak concentration. Most of laboratory simulations have values of $-0.50 \leq FB \leq -0.25$ and $0.35 \leq NMSE \leq 0.70$. Hanna [1990] evaluated fourteen numerical hazardous gas models using data from the Desert Tortoise ammonia (NH_3) and Goldfish hydrogen fluoride (HF) field experiments. His data suggest that there is a cluster of eight models with relatively good performance with values between $-0.4 \leq FB \leq 0.0$ and $0.25 \leq NMSE \leq 0.50$. The numerical models also underpredict field concentrations. Figure 5 shows a plot of NMSE vs. FB for arrival time of concentration with a magnitude of 20 percent of $\bar{C}_{MAX}$. Most FB values fall within a range of $\pm$ 0.38 and $0.0 \leq NMSE \leq 0.4$. NMSE and FB values for arrival time of $\bar{C}_{MAX}$ are within a range of $\pm$ 0.30 and $0.0 \leq NMSE \leq 0.45$.

The NSME vs FB figure does not suggest there is a specific relation between a length scale and performance, but values for both 20% and $\bar{C}_{MAX}$ arrival times suggest that the performance improves as the length scale decreases. The figures also show that Freon-12 simulant gas predicts the field data better than Argon gas. Both trends suggest that improvement in plume Reynolds number magnitude is desirable. Meroney (1986) predicted such trends would occur as Peclet/Richardson ratio and Reynolds numbers increase.

3.2 Surface Pattern Comparisons of Specific Laboratory/Field Data

One objective of this wind-tunnel program was to determine how accurately physical modeling replicates field conditions. For most model performance measures, the instantaneous predicted values are directly compared to measured values. However, the spatial distribution of plume concentrations appears to be more critical than the temporal distribution for LNG hazard assessment. Lewellen and Sykes [1985] proposed a measure of the spatial comparison between observed and predicted patterns, which compares data over increments of decreasing spatial resolution. It estimates how much the predicted pattern must be shifted in space to cover all of the observed values.

This method considers the segment of area $A(x_o, \delta\theta)$ sketched in Figure 6, centered on the observation point and bounded by an angular displacement, $\delta\theta$, relative to the source point. The area is bounded by $\theta_i + \delta\theta$, $\theta_i - \delta\theta$, $r_i(1+\delta\theta)$, and $r_i(1-\delta\theta)$. Within this area the predicted concentration is bounded by lower and upper values defined as $C_p^{\,l}(A)$ and $C_p^{\,u}(A)$, respectively. Given observed concentrations $C_o(x_i)$ at a number of points i = 1, 2, 3,..., M, the effective predicted concentrations for the area A is defined in terms of the two limiting values, $C_p^{\,l}$ and $C_p^{\,u}$, and the observed concentration $C_o(x_i)$ as the following:

$$C_p(x_i, \delta\theta) = \begin{cases} C_p^{\,l}(A) & \text{if } C_o(x_i) < C_p^{\,l}(A) \\ C_o(x_i) & \text{if } C_p^{\,l}(A) < C_o(x_i) < C_p^{\,u}(A) \\ C_c^{\,u}(A) & \text{if } C_o(x_i) > C_c^{\,u}(A) \end{cases}$$

The ratio used for comparison is defined as

$$N_i = \begin{cases} C_p(x_i, \delta\theta)/C_o(x_i) & \text{if } C_p(x_i, \delta\theta) \geq C_o(x_i) \quad \text{or} \\ C_o(x_i)/C_p(x_i, \delta\theta) & \text{if } C_p(x_i, \delta\theta) < C_o(x_i) \end{cases}$$

Thus, the comparison is not between the observed and predicted concentration at a point, but rather between the observed concentration at a point and the calculated concentration for the area

A. One can now calculate the fraction of the test points, $f_N(\delta\theta,N)$, which yield predicted concentrations within a specified ratio N of the observed values within the areas defined by δA.

$$f_N(\delta\theta,N) = \frac{1}{M} \sum_{i=1}^{M} H\{ N - N_i \}$$

where $H\{f\} = 1$ if $f \geq 0$

$= 0$ if $f < 0$.

A plot of $f_N(\delta\theta,N)$ gives a direct measure of how well the laboratory-predicted spatial distribution compares with the observations. Thus, one can plot the sequence of curves $f_N(\delta\theta,N)$ as a function of $\delta\theta$ for a various values of N.

Falcon 4 test data were compared to laboratory data, and pattern comparison factors were calculated. Figures 7 and 8 are plots of f-N vs. Degree with specified pattern factors for different run conditions. Figure 7 shows that 100 percent of the observations are covered by a shift of 15° for N = 1 and the shift decreases to 7° for N = 2 with Argon gas. For Freon-12 gas the shift needed to cover the observations increases to 20° and 8° for N = 1 and 2, respectively. However, one can not say that Argon gas has better spatial prediction than Freon-12 gas since both gases were not compared with the same model scales. Contours of peak concentrations used to determine the pattern factor were made with data for a length scale of 100 with Argon and length scales of 150 and 200 with Freon-12, since concentrations were measured at only two different downwind distance for other length scales for Falcon 4 simulations. Pattern comparison test summary bar charts are also shown in Figure 9 and Figure 10. These figures show that the pattern factor increases as the length scale ratio decreases, suggesting that the model predicts the observations better spatially as the model size increases.

3.3 Depth-Averaged Numerical Model

The Falcon tests release denser-than-air gas for a finite time from an area surrounded by fences and a vortex generating barrier. A depth-integrated quasi-three-dimensional model (DENSE20) was developed to calculate the behavior of heavy and cold gas clouds released into the atmosphere at ground level [Meroney, 1984]. The effect of a fence on plume dispersion located in downwind of a source area was included in a model called FENC23 [Meroney et al., 1988]. In this study FENC23 was expanded to include the effects of fences located upwind and downwind of the source area. The Pe_*/Ri_* ratio for laboratory tests ranged from 0.07 to 0.001 implying that the model tests might underpredict peak concentrations. (Underprediction occurs because microscopic diffusivity exceeds the modeled turbulence diffusivities in such circumstances.) Thus, Pe_*/Ri_* effect was examined for cases with fences and without a fence. Numerical calculations confirm that the plume dispersion was significantly influenced by microscopic diffusion when a fence is not present, however the effect of Pe_*/Ri_* ratio change is not significant when fences are included.

Figure 11 shows a peak concentration decay comparison between different fence schemes. Ensembles of peak concentrations for five repetitions, peak of maximum model concentrations and field data were compared to numerical predictions. The figure shows that the numerical model predicts field data and wind-tunnel data fairly well.

4. Conclusions

1. The Pe_*/Ri_* ratio is not critical in laboratory simulations when obstacles are present. Thus, fluid modeling of dense gas dispersion in the presence of industrial complexes should not substantially underpredict anticipated spill concentrations.

2. Peak concentrations of field data and post-field wind-tunnel simulations agreed within a range of $-0.50 \leq FB \leq -0.25$ and

$0.35 \leq$ NMSE ≤ 0.70 for most simulations. Arrival times of $0.2\bar{C}_{MAX}$ have FB values within ± 0.38 and $0.0 \leq$ NMSE ≤ 0.4. The arrival time of $\bar{C}_{MAX}$ have FB values in a range of $\pm$ 0.30 and $0.0 \leq$ NMSE ≤ 0.45. Thus, fluid modeling predicts dense gas dispersion in the vicinity of industrial complexes well within the accuracy required for hazard site evaluation.

3. The use of Freon-12 simulant gas improved model predictions of field plume concentrations by about 20 percent. Hence, distorted density modeling of heavy gas spills will generally improve model accuracies. This improvement is primarily due to improved simulation of wake behaviors resulting from increased model Reynolds numbers.

4. Comparison of visual plume data recorded on VCR tapes suggested that the plume had more turbulence and dispersed more quickly in the wind tunnel than in the field.

References

[1] Meroney, R. N. (1984), " Transient Characteristics of Dense Gas Dispersion; Part I: A Depth-Averaged Numerical Model," J. of Hazardous Materials, Vol. 9, pp. 139-157.

[2] Meroney, R.N. (1986), "Guideline for Fluid Modeling of Liquified Natural Gas Cloud Dispersion - Vol. II:," Technical Support Document, Final Report for Gas Research Institute, Report GRI86/0102.2, 262 pp.

[3] Meroney, R.N., Neff, D.E., Shin, S.H., Steidle, T.C., Tan, T.Z., and Wu, G. (1988), "Analysis of Vapor Barrier Experiments to Evaluate their Effect as a Means to Mitigate the HF Cloud Concentration," for Exxon Research and Engineering, Florham Park, New Jersey, CSU Contract No.

29-7330, CER88-89RNM-DEN-SHS-TCS-TZT-GW-1, 200 pp.

[4] Neff, D.E. and Meroney, R.N. (1986), "LNG Vapor Barrier and Obstacle Evaluation: Wind-Tunnel Pre-Field Test Results," for Lawrence Livermore Laboratory, Contract No. 8432705, FMWEP85-86RNM3.

[5] Hanna, S.R., Strimaitis, D.G., and Chang, J.C. (1990), "Evaluation of 14 Hazardous Gas Models with Ammonia and Hydrogen Fluoride Field Data," for Submittal to Journal of Hazardous Materials.

[6] Ermak, D.L. and Merry, M.H. (1988), "A Methodology for Evaluating Heavy Gas Dispersion Models", 88 pp.

[7] Lewellen, W.S. and Sykes, R.I. (1985), "A Scientific Critique of Available Models for Real-Time Simulations of Dispersions," Nuclear Regulatory Commission Report NUREG/CR-4157.

[8] Brown, T.C., Cederwall, R.T., Ermak,D.L., Koopman, R.P., McClure, J.W., and Morris, L.K. (1988), "Falcon Series Data Report: 1987 LNG Vapor Barrier Verification Field Trials".

Table 1 Wind-Tunnel Tests Conducted

Test	Length Scale	Source Combination	Array Angle	Locations Tests Argon	Freon-12	Angle Change	Source Change
Falcon 1	50			X(a)			
	100			X(b)			
	150			X(c)			
	200			X(d)			
Falcon 2	50	10% S + 90% P	225°T	114			
	100	50% S + 50% P	225°T	161			
	150	100% S	225°T	161			
	200	100% S	225°T	90			
Falcon 3	50			X(e)			
	100	70% S + 30% P	225°T	161			
	150	50% S + 50% P	225°T	105			
	200	70% S + 30% P	225°T	77			
Falcon 4	50	90% S + 10% P	235°T	114		225°T	
	100	70% S + 30% P	235°T	161		225°T	
	150	70% S + 30% P	235°T	116	132	225°T	
	200	70% S + 30% P	235°T	88	90	225°T	
	100	100% S				225,232°T	
	100		225°T				YES
Falcon 5	50			X			
	100	70% S + 30% P	225°T	161			
	150	50% S + 50% P	225°T	90			
	200	50% S + 50% P	225°T	77			

Locations Tested: Measurement locations (Repetitions - 5 times each)
S: Spider
P: Plenum
X: No experiment
X(a) - X(d): Wind velocity was too low to simulate in EWT.
X(e) :Gas flow rate was too large to supply through model source tube

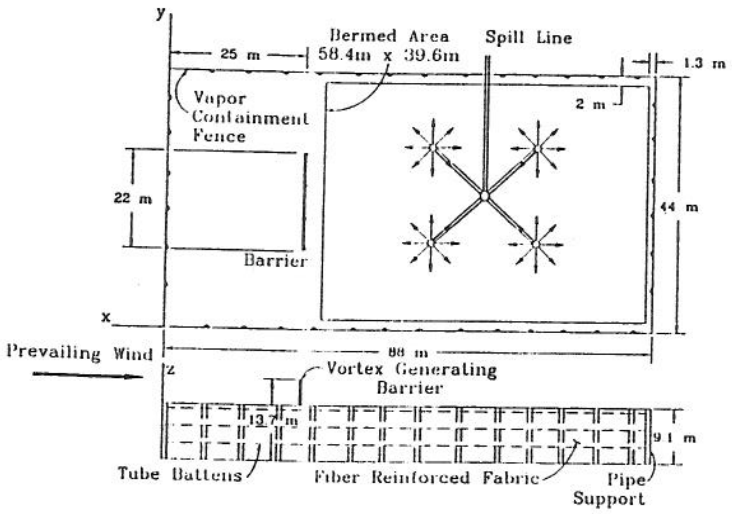

Figure 1 Field test facility

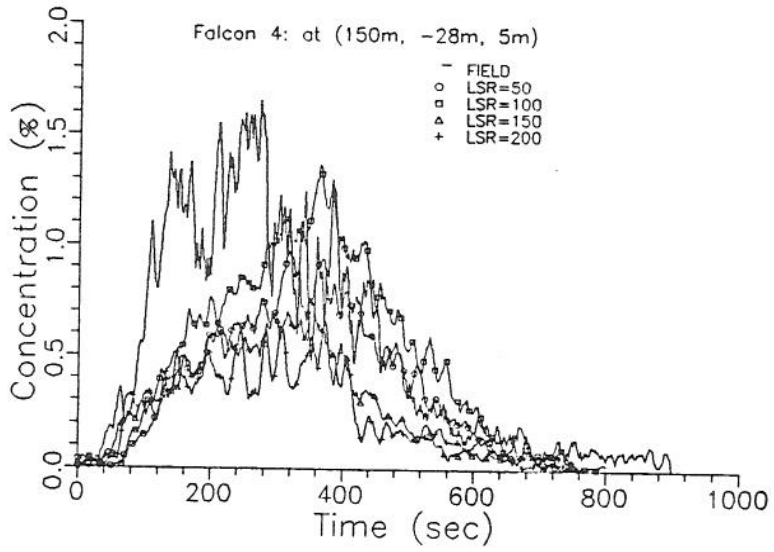

Figure 2 Concentration time history comparison between all model scales for Falcon 4

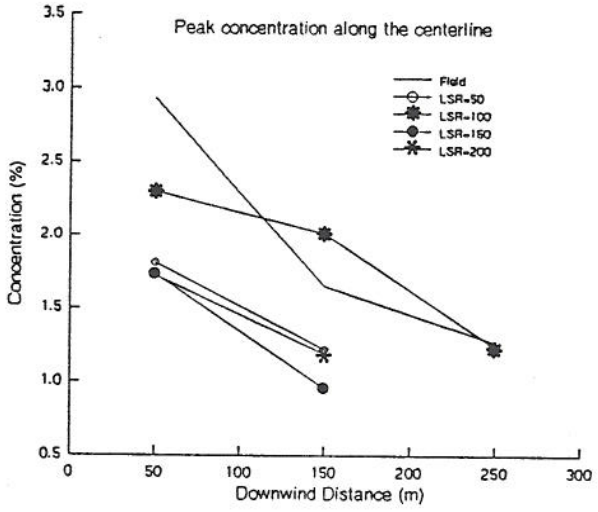

Figure 3 Peak centerline concentration comparison for all model scales for Falcon 4 simulations at z=5 m

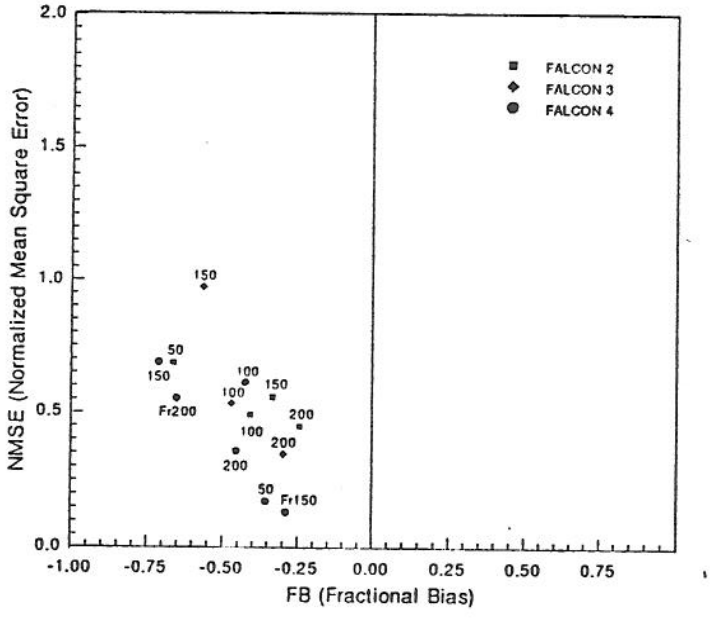

Figure 4 Weighted average Fractional Bias, FB, and Normalized Mean Square Error, NMSE, for peak concentration predictions for Falcon experiments 2 to 4

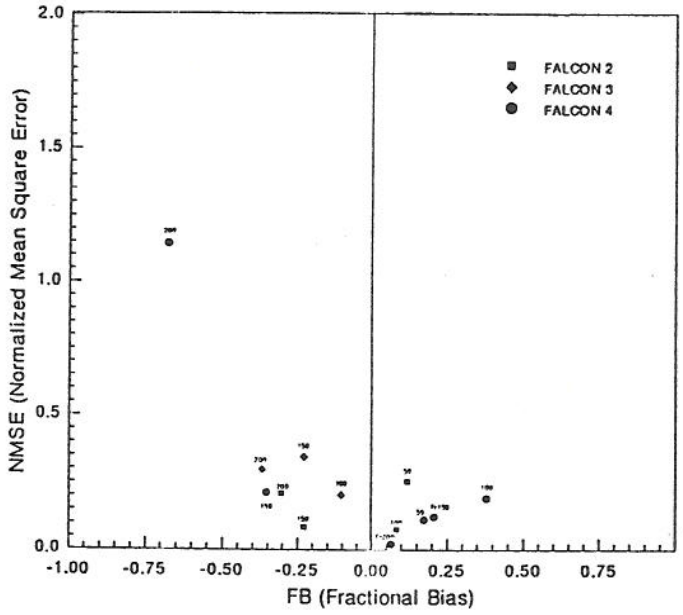

Figure 5 Weighted average Fractional Bias, FB, and Normalized Mean Square Error, NMSE, for arrival time predictions for Falcon experiments 2 to 4

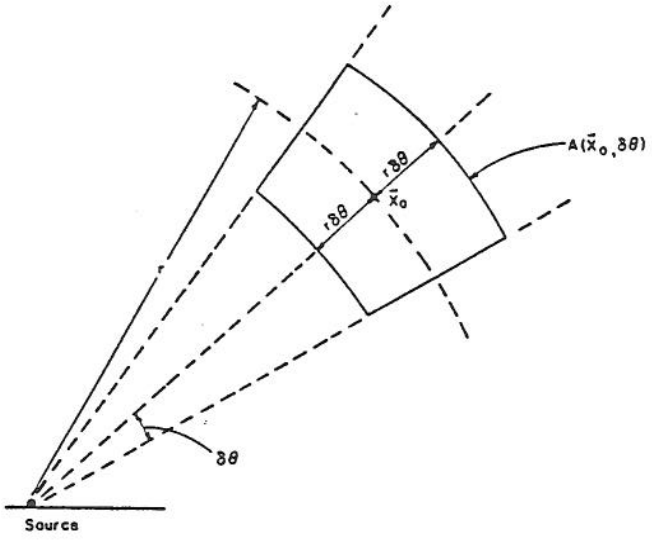

Figure 6 Schematic of the Area Segment, $A(x_i, \alpha\theta)$

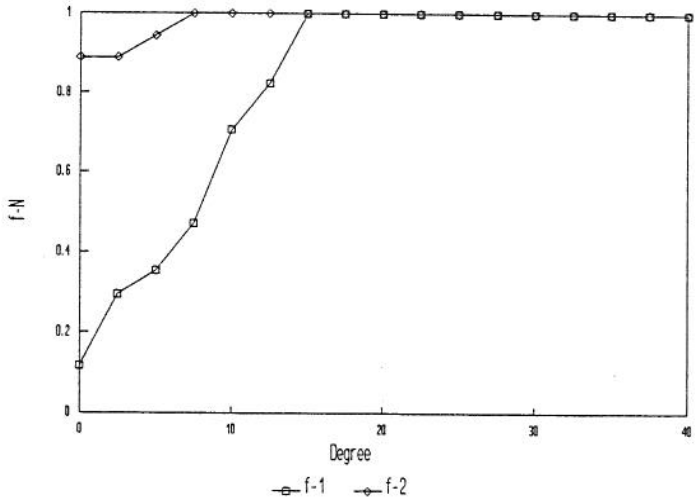

Figure 7 Pattern comparison plot: Falcon 4 (Argon), LSR=100, z=5 m

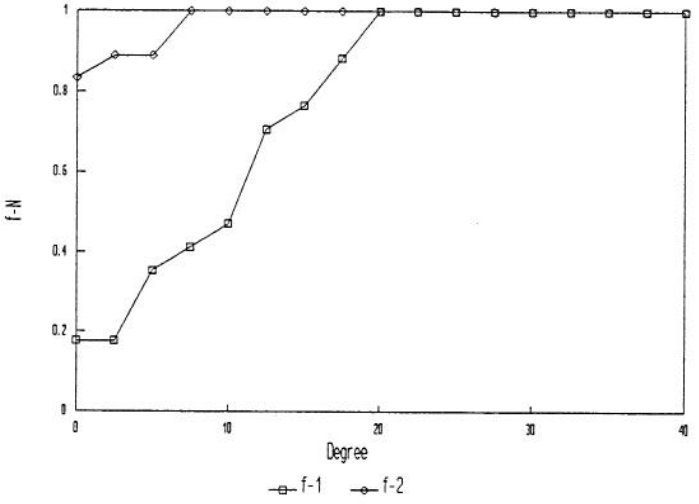

Figure 8 Pattern comparison plot: Falcon 4 (Freon-12), LSR=150, z=5 m

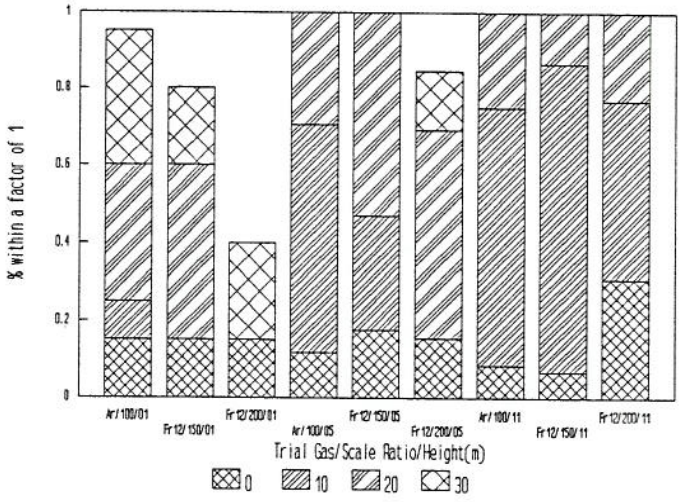

Figure 9 Pattern comparison test summary bar chart for % compatibility of factor 1 at θ angles between 0° and 30°

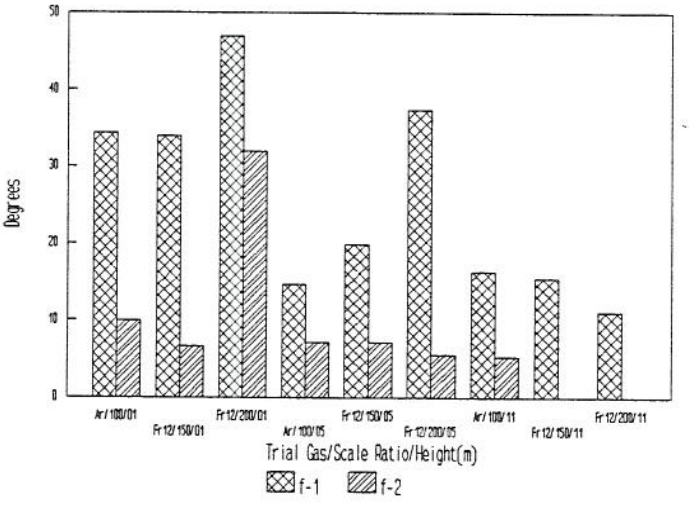

Figure 10 Pattern comparison test summary bar chart for θ intercept (degrees)

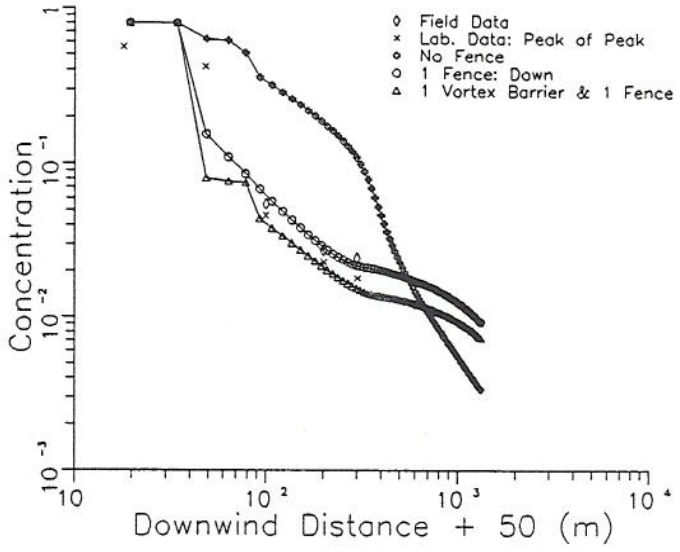

Figure 11 Peak concentration comparison between different fence schemes: $C_D = 0.10$